ELSEVIER

Polymer 44 (2003) 467–471

polymer

www.elsevier.com/locate/polymer

Effects of matrix viscoelasticity on drop deformation in dilute polymer blends under slow shear flow

S. Guido[a,*], M. Simeone[a], F. Greco[b]

[a]*Dipartimento di Ingegneria Chimica, Università di Napoli 'Federico II', Piazzale Tecchio 80, I-80125 Napoli, Italy*
[b]*Istituto per la Tecnologia dei Materiali Compositi (ITMC)—CNR, Piazzale Tecchio 80, I-80125 Napoli, Italy*

Abstract

The deformation of a single drop in a flowing dilute polymer blend is here investigated for slow steady shear, through video-enhanced microscopy and image analysis. The data are interpreted in terms of a perturbative solution of the fluidodynamic problem for small drop deformations, where effects of matrix viscoelasticity are taken into account. It is found that drop orientation towards the shear direction is directly linked to normal stresses in the matrix fluid.

Keywords: Polymer blend; Drop deformation in shear flow; Normal stresses

1. Introduction

Liquid–liquid dispersed systems, such as emulsions or polymer blends, are 'complex fluids', typically encountered in a variety of applications, including, e.g. cosmetics design, food processing, and plastics technology [1]. It is well-known (and intuitively understood) that many physical properties of these systems are strongly influenced by morphology, i.e. size and shape of the dispersed phase inclusions. Control of morphology under the flow conditions experienced in processing is therefore an essential task, which has also generated a basic scientific interest in the fluidodynamics of these liquid–liquid suspensions.

Most studies in this field, both theoretical and experimental, dealt with Newtonian component fluids, starting from the fundamental pioneering contributions by Taylor on the flow-induced small deformation of a single droplet and on the viscosity of dilute emulsions [2,3]. Later works were devoted to the rheological behavior of these systems at higher concentration of the dispersed phase [4,5] and to the case of large drop deformations up to break-up [6]. It so appears that even though some problems still remain open (such as coalescence [1]), a reasonable understanding of the Newtonian case has been reached.

On the other hand, a comparably clear picture does not emerge from the literature for the case where one or both the blend components are non-Newtonian fluids, in spite of its practical relevance. Because of the lack of theoretical treatments, the rather sparse experimental results on these systems [7–9] are of difficult interpretation. As an example, it is not known how the flow-induced morphology of a polymer blend is related to the non-Newtonian properties of the component polymers, such as shear-rate dependent viscosity, and normal stresses. In view of this situation, it is apparent that the basic rheological effects associated with viscoelasticity of the component fluids are best explored in the simplest possible case, i.e. that of a single droplet in a well-controlled flow field (the 'infinite dilution' limit).

In this Communication, we report on the case of a drop in simple shear flow. The matrix phase of the blend is viscoelastic, whereas drops are made of a Newtonian fluid. Drop deformation is investigated in a parallel plate apparatus, equipped with video optical microscopy, and the experimental results are compared with predictions of a recently developed perturbative calculation for small drop deformations [10].

2. Experimental part and theoretical analysis

2.1. Apparatus

In Fig. 1, a 'side-view' of a deformed drop under shear flow between parallel plates is sketched. The x-axis is along the flow direction 'at infinity', and the shear gradient direction y is normal to the plates. The major and minor

* Corresponding author. Tel.: +39-081-7682271; fax: +39-081-2391800.
E-mail address: steguido@unina.it (S. Guido).

0032-3861/03/$ - see front matter © 2002 Published by Elsevier Science Ltd.
PII: S0032-3861(02)00763-2

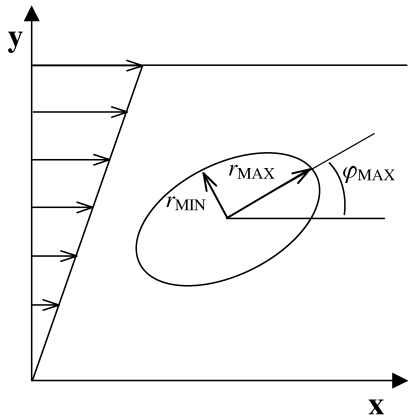

Fig. 1. The reference system and the geometric quantities used to describe drop deformation under shear flow between parallel plates.

axes, r_{MAX} and r_{MIN}, respectively, of the (projected) drop, and the orientation angle φ_{MAX} between r_{MAX} and the x-axis are also shown in Fig. 1. These geometrical quantities, which are rather easy to measure, will be used here to describe drop contour in the shear plane.

A detailed description of the apparatus used to study drop deformation can be found elsewhere [11,12]. Briefly, simple shear flow is generated in a parallel plate device, equipped with a video-enhanced contrast microscopy and imaging system. In the setup used in this work, the drops are observed along the z-axis (i.e. the 'vorticity' direction of the shear flow) by using as parallel plates a couple of glass bars of square section, (100 mm × 50 mm × 50 mm), each glued on a glass slide, which fits in a window cut on a rigid mount. Parallelism between the two plates is adjusted by a set of micrometric rotary and tilting stages (the residual error is around 20 μm over a length of 10 cm). Shear flow at a constant shear rate $\dot{\gamma}$ is obtained by translating one of the plates at a constant speed with respect to the other, through a computer-controlled motorized translating stage with micrometric precision. A few drops (typical rest radius r_0 is around 50 μm) are injected in the continuous phase, preliminarily loaded between the parallel plates, by a tiny glass capillary, fixed to a home-made micromanipulator. The microscope is also mounted on a separate motorized translating stage, which is used to keep the deforming drop within the field of view during motion. Quantitative analysis of drop shape is performed by an automated image analysis edge-detection procedure.

2.2. Theoretical analysis

The main mathematical difficulties of the 'drop in a flow field' problem is that a part of the boundary conditions to be satisfied (velocity continuity, normal stress balance, etc.) is assigned on the surface of the deforming drop, which is itself unknown. A perturbation approach, i.e. by considering the limit of small deformations around the spherical shape, is therefore the only available route to get analytical results [2,10,14].

To these days, perturbative calculations have been developed for Newtonian fluids only. Quite recently, the perturbation problem, for the non-Newtonian case, has been tackled by one of us (Greco, [10]), with the component fluids obeying the 'second-order fluid' constitutive equation [15]. The new perturbative calculations therefore account for the constitutive elasticities (normal stresses) of the component fluids.

It is readily shown in this case that apart from purely constitutive coefficients (such as the viscosity ratio λ of the drop to the continuous phase, or the ratio of second to first normal stress differences), two non-dimensional groups arise. One of them, namely, $r_0\eta\dot{\gamma}/\sigma$, where η is the matrix viscosity and σ is the interfacial tension, is the so-called capillary number Ca, which suffices in the Newtonian case. The other one, namely, $W = r_0N_1/2\sigma$, where N_1 is the matrix first normal stress difference, is a non-dimensional number giving the ratio of elastic to interfacial stress, hence is the natural non-Newtonian counterpart of the capillary number Ca (ratio of viscous to interfacial stress).

The perturbation procedure worked out in Ref. [10] adopts the non-dimensional numbers Ca and W as the expansion parameters. Indeed, the conditions of small Ca and W correspond to small drop deformations from the unperturbed spherical shape, because interfacial forces are dominant. A double asymptotic expansion in Ca and W can then be performed, generating a hierarchy of fluidodynamic problems, at order Ca and Ca^2 (the Newtonian case), and at order W (the non-Newtonian problem). Details of calculations have been reported elsewhere [10].

It is understood that although both Ca and W must be small to stay in the small deformation limit, they should be comparable in magnitude, i.e. $p = W/Ca^2 \geq 1$, in order to make the non-Newtonian constitutive contributions measurable. In other words, we envisage that the appropriate condition to be satisfied is:

$$\eta^2\dot{\gamma}^2 \leq \frac{\sigma}{r_0}N_1 \tag{1}$$

while Ca stays at a low value. From Eq. (1), we infer that by appropriately choosing an highly elastic matrix (e.g. a 'Boger fluid' [16]), non-Newtonian effects on drop shape should become observable under slow flow conditions. The validation of such prediction is, in fact, the purpose of the present Communication.

2.3. Materials

On the basis of the analysis of Section 2.2, the polymers for the experiments were chosen as follows. The drop phase is a silicon oil (Dow Corning 200/12500 cS), displaying Newtonian behavior with a viscosity of 13 Pa s at 25 °C. The matrix is a Boger fluid made of corn syrup with 0.13 wt% high molecular weight polyacrylamide (PAA, trade name: Separan AP 30). In the range of shear rate investigated (up to 20 s^{-1}), the matrix viscosity is almost

constant (10 Pa s at 25 °C), and a significant first normal stress difference can be measured (the first normal stress coefficient $\psi_1 = N_1/\dot{\gamma}^2$ was fitted to be 2.5 Pa s^2 in the $\dot{\gamma}$ range 2–20 s^{-1} where reliable N_1 data could be measured). The rheological data were obtained by using a constant-stress rheometer (Bohlin, CVO 120) in the cone-and-plate configuration. The two selected fluids are essentially immiscible, as shown in separate experiments where undeformed drop size was monitored as a function of time, and no significant change was observed. The interfacial tension of the liquid pair is measured by a standard experimental procedure [13,17,18], and is ca. 30 mN/m. Finally, buoyancy effects on the injected drop were found to be negligible, as expected because of the high viscosities and the small density difference between the two liquids. From the just given rheological and interfacial data, we calculate $\lambda = 1.3$ and $p = 6.3$. From the latter value, significant non-Newtonian effects on drop shape are expected, due to the first normal stress difference in the matrix fluid.

3. Results and discussion

The theoretical predictions under the conditions reported in Section 2.3 show negligible deviations of the major and minor axis of the drop from the corresponding Newtonian case (i.e. with the same viscosity ratio). Conversely, the calculated trend of the angle φ_{MAX} when varying the capillary number is quite different from the Newtonian case. In the following, we will show how our experimental results do confirm these predictions.

In Fig. 2, typical (side view) micrographs of drops deformed under shear flow are presented. The top image corresponds to the non-Newtonian system silicon oil in corn syrup with PAA, as described above. The lower image, conversely, corresponds to a Newtonian system (polydimethylsiloxane in polyisobutilene), i.e. with both fluids having constant viscosity and unmeasurable normal stresses. The capillary number *Ca* and the viscosity ratio λ are close in the two images (in the Newtonian system, it is $\lambda = 1.1$). Nevertheless, a marked difference in the orientation of the drop is apparent, as anticipated. In the non-Newtonian case, the drop is much more aligned to the flow direction, though its deformation looks quite alike that of the drop in the Newtonian system.

In Fig. 3, the measured non-dimensional major and minor axis r_{MAX} and r_{MIN}, respectively, are plotted as a function of the capillary number *Ca* for our non-Newtonian system. Lines are predictions from the perturbative theory, in the Newtonian ($p = 0$; dashed line) and non-Newtonian ($p = 6.3$; solid line) case, both at $\lambda = 1.3$. Data somehow fall in between the two lines. Accounting for measuring uncertainty, it may be stated that the non-Newtonian constitutive behavior of the matrix fluid has essentially no influence on drop shape, at least at small deformations. Note

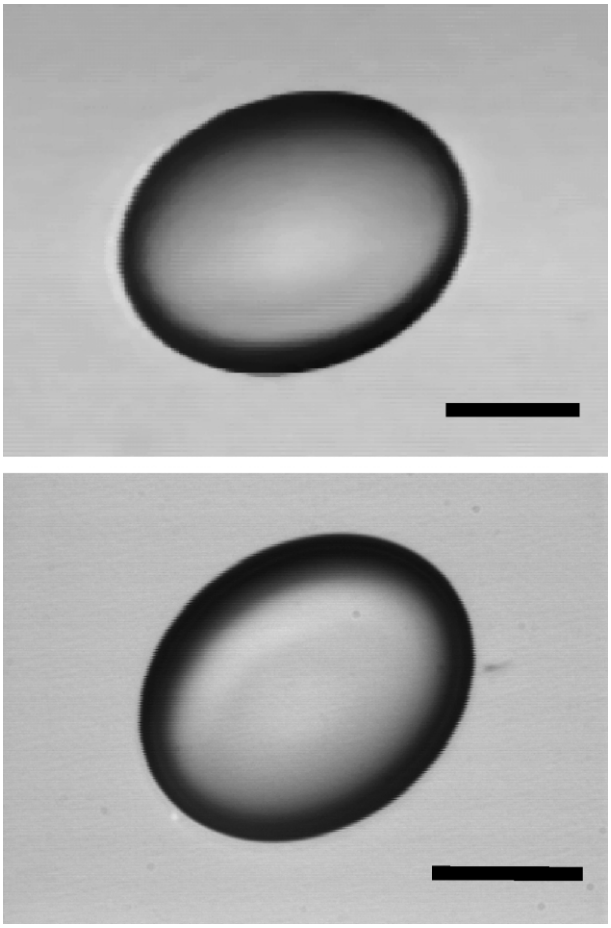

Fig. 2. Video-enhanced microscopy images of deformed drops under shear flow at similar values of *Ca* and λ (bar length = 50 μm). Top and bottom image correspond to a non-Newtonian and a Newtonian matrix, respectively, (see text).

in this respect that even at the maximum *Ca* in Fig. 3, the percent difference between the major and minor axis and the drop radius at rest is around 10%.

In Fig. 4, the orientation angle φ_{MAX} of the deformed drop is plotted as a function of the capillary number. Data points refer to the non-Newtonian system. An indicative

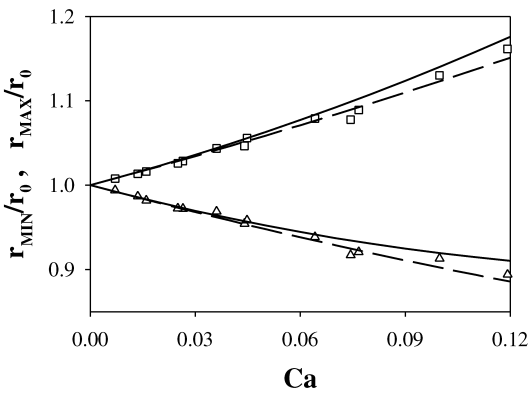

Fig. 3. Non-dimensional r_{MAX} and r_{MIN} vs. capillary number *Ca*. Dashed lines are Newtonian predictions ($\lambda = 1.3$), solid lines are non-Newtonian predictions ($p = 6.3$, $\lambda = 1.3$).

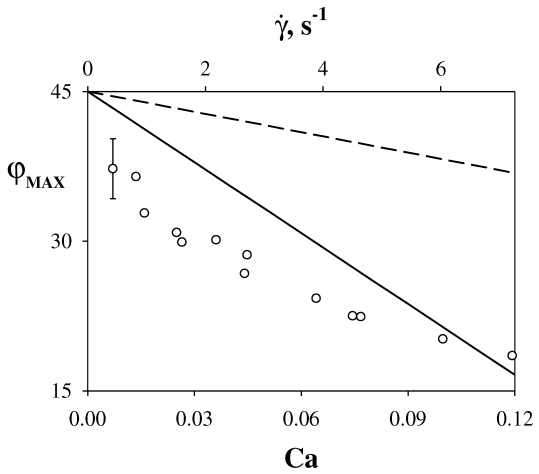

Fig. 4. Angle φ_{MAX} vs. capillary number *Ca* (bottom axis) and $\dot{\gamma}$ (top axis). As in Fig. 3, dashed lines are Newtonian predictions ($\lambda = 1.3$), solid lines are non-Newtonian predictions ($p = 6.3$, $\lambda = 1.3$).

error bar, representing the standard deviation of the measurements, is placed on the first data point only, where the experimental uncertainty in the angle is larger (due to the difficulty of measuring drop orientation for very small deformations). The lines in Fig. 4 are obtained from the following equation

$$\varphi_{MAX} = \frac{\pi}{4} - [f_1(\lambda) + f_2(\lambda)p]Ca \tag{2}$$

which is deduced from the perturbation theory [10], with

$$f_1(\lambda) = \frac{(3 + 2\lambda)(16 + 19\lambda)}{80(1 + \lambda)} \tag{3}$$

$$f_2(\lambda) = \frac{176 + \lambda(436 + 323\lambda)}{30(1 + \lambda)(16 + 19\lambda)} \tag{4}$$

(The second normal stress difference of the matrix fluid, if any, is ineffective in Eq. (2)). Dashed and solid line refer to the Newtonian and non-Newtonian case, respectively. A marked difference between the two cases is here apparent, at variance with the findings for the drop axes (Fig. 3).

The non-Newtonian prediction for the angle in Fig. 4 is clearly supported by the experimental data, although some scatter is present. It should be noted in this respect that the p value used in Eq. (2) ($p = 6.3$) was obtained by fitting N_1 data in the $\dot{\gamma}$ range 2–20 s^{-1}, whereas the angle φ_{MAX} was determined in the $\dot{\gamma}$ range 0–7 s^{-1}, hence some discrepancy between predictions and experiments in Fig. 4 is expected. It can, however, be seen that in a sheared non-Newtonian matrix, the steady state angle between the drop major axis and the flow direction is significantly lowered with respect to the corresponding Newtonian case. To our knowledge, this result is reported here for the first time.

In a recent paper, dealing with a (quasi) Newtonian drop in a viscoelastic matrix, Mighri et al. [8] found a a marked, positive deviation of the 'drop deformation' from the Newtonian case (Fig. 3). The drop deformation parameter used in Ref. [8] is the ratio between the projected major axis of the drop and the diameter at rest. We see then that Mighri et al. findings are in qualitative agreement with the results presented here. Indeed, since we found that the angle between the drop major axis and the shear direction is lowered with respect to the Newtonian case, the projected major axis is higher than in the Newtonian case. Of course, since in Ref. [8] only the view along the velocity gradient was available, it was not possible in their work to discriminate between a drop deformation increase and the orientational increase. We argue that the deformation increase is in fact only apparent, the real physical effect being the orientational increase, as observed in our view along the vorticity axis.

Experimental determination of normal stresses is a difficult task in rheometry. We have shown here that normal stress measurements can in fact be related to accurate optical observations of drops in flow, by using the small deformation theory for second-order fluids blends (Eq. (2)). In principle, the complete rheological characterization of a fluid (under slow flows) can be obtained by exploitation of our experimental apparatus and of the small deformation theory [10], once the properties of the partner fluid of the blend are separately known. It should be also mentioned that in order to perform the measurements with our apparatus, tiny quantities of fluids are required (the gap volume between the plates is typically 0.25 ml), which is a desirable feature in all the cases when sample amounts are limited.

4. Conclusion

In summary, we have studied the problem of a single drop in shear flow for the case of a viscoelastic matrix. Rheo-optical experiments were performed, and detailed measurements of drop shape by video microscopy and image analysis were compared to predictions from a perturbative theory. The main result of this Communication is that drop orientation under flow is directly related to normal stresses of the matrix fluid, thus linking optical and rheological measurements. Further work is in progress to systematically investigate non-Newtonian effects on drop deformation by varying the properties of the blend components.

Acknowledgements

This work is supported by the Italian National Research Council (CNR).

References

[1] Larson RG. The structure and rheology of complex fluids. New York: Oxford University Press; 1999.
[2] Taylor GI. Proc R Soc Lond 1932;A138:41.

[3] Taylor GI. Proc R Soc Lond 1934;A146:501.
[4] Han CD. Multiphase flow in polymer processing. New York: Academic Press; 1981.
[5] Yang H, Zhang H, Moldenaers P, Mewis J. Polymer 1998;39:5731.
[6] Stone HA. Ann Rev Fluid Mech 1994;26:65.
[7] Levitt L, Macosko CW, Pearson SD. Polym Engng Sci 1996;36:1647.
[8] Mighri F, Carreau PJ, Ajji A. J Rheol 1998;42:1477.
[9] Hobbie EK, Migler KB. Phys Rev Lett 1999;82:5393.
[10] Greco F. J nonNewt Fluid Mech 2002:107:111.
[11] Guido S, Simeone M. J Fluid Mech 1998;357:1.
[12] Guido S, Villone M. J Rheol 1998;42:395.
[13] Sigillo I, Di Santo L, Guido S, Grizzuti N. Polym Engng Sci 1997;37:1540.
[14] Barthes-Biesel D, Acrivos A. J Fluid Mech 1973;61:1.
[15] Astarita G, Marrucci G. Principles of non-Newtonian fluid mechanics. Maidenhead: McGraw-Hill; 1974.
[16] Boger DV, Binnington R. Trans Soc Rheol 1977;221:515.
[17] Rumscheidt FD, Mason SG. J Colloid Interface Sci 1961;16:238.
[18] Torza Z, Cox RG, Mason SG. J Colloid Interface Sci 1972;38:395.